Nanoscale Advances

ROYAL SOCIETY OF CHEMISTRY

MINIREVIEW

View Article Online
View Journal | View Issue

Check for updates

Cite this: *Nanoscale Adv.*, 2023, **5**, 313

Recent advances in epitaxial heterostructures for electrochemical applications

Tong Bao,[b] Jing Wang*[ab] and Chao Liu *[b]

Construction of epitaxial heterostructures is crucial for boosting the electrochemical properties of various materials, however a review dedicated to this attractive topic is still lacking. In this Minireview, a timely summary on the achievements of epitaxial heterostructure design for electrochemical applications is provided. We first introduce the synthesis strategies to provide fundamental understanding on how to create epitaxial interfaces between different components. Secondly, the superiorities of epitaxial heterostructures in electrocatalysis, supercapacitors and batteries are highlighted with the underlying structure–property relationship elucidated. Finally, a discussion on the challenges and future prospects of this field is presented.

Received 15th October 2022
Accepted 29th November 2022

DOI: 10.1039/d2na00710j

rsc.li/nanoscale-advances

Open Access Article. Published on 29 11 2022. Downloaded on 2026-06-01 2:54:26.
This article is licensed under a Creative Commons Attribution-NonCommercial 3.0 Unported Licence.

1. Introduction

Climate warming and environmental pollution caused by the wide use of traditional fuels are urgent global concerns, constantly provoking the development of clean and renewable energy resources.[1–3] Hydrogen is regarded as a perfect energy carrier with higher energy density (120 MJ kg^{-1}) than gasoline (44 MJ kg^{-1}), while producing no harmful chemicals.[4–7] In addition, a variety of electrochemical energy storage and conversion technologies such as water splitting,[8–11] supercapacitors[12–14] and batteries[15–18] are also highly promising for addressing the energy issues. The key to achieve high performances is the rational design of electrode materials with optimal structures and compositions to facilitate the reactions and/or electron/mass transport during the energy conversion/storage processes.[19–21] Sustainable research attention has thus been paid to the identification of functional electrode materials including carbon-based materials (*e.g.* graphene,[22] carbon nanotubes[23] and porous carbon nanostructures[24]), metal compounds (*e.g.* metal oxides,[25] hydroxides,[26] sulfides,[27] phosphides[28] and selenides[29]), *etc.* However, these single component materials suffer from limitations in the regulation of electronic structures and electrochemical reaction interfaces; both of these parameters are crucial for determining the ultimate performances.

To further boost the electrochemical properties, construction of heterostructures by integrating two or more components especially with small lattice mismatch less than 15% at the interface, named epitaxial heterostructures (EHs), is a fascinating strategy and has received extensive attention.[30–34] The architectures, compositions and functionalities of EHs can be

[a]*School of Chemical and Environmental Engineering, Shanghai Institute of Technology, Shanghai 201418, P. R. China. E-mail: jingwang@sit.edu.cn*
[b]*School of Chemistry and Molecular Engineering, East China Normal University, Shanghai 200241, P. R. China. E-mail: cliu@chem.ecnu.edu.cn*

Tong Bao received her Bachelor degree from East China Normal University under the supervision of Prof. Chengzhong Yu and Prof. Chao Liu in 2022. She is currently a postgraduate student under the supervision of Prof. Chao Liu at East China Normal University. Her research field is the synthesis of MOF-based nanostructures for applications in catalysis.

Jing Wang received her Ph.D. degree (2018) from Nanjing University of Science and Technology. She worked as a postdoctoral fellow in Prof. Chengzhong Yu's group at East China Normal University (2018–2022). She is currently an associate professor at Shanghai Institute of Technology. Her research focuses on the design of functional nanomaterials for environmental remediation and electrocatalysis.

© 2023 The Author(s). Published by the Royal Society of Chemistry

Open Access Article. Published on 29 11 2022. Downloaded on 2026-06-01 2:54:26.
This article is licensed under a Creative Commons Attribution-NonCommercial 3.0 Unported Licence.

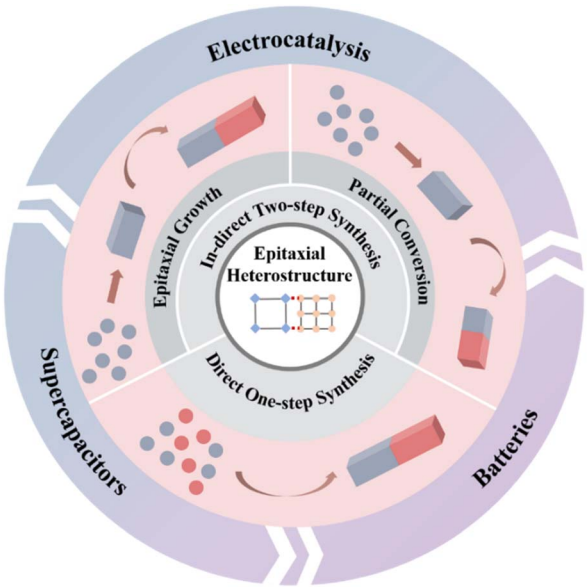

Scheme 1 Illustration of the synthesis and electrochemical applications of EHs.

facilely tuned by adjusting the coupling ways of different subunits. Compared to traditional heterostructures with large lattice mismatch, EHs generally exhibit an intimate interface with different materials closely connected at the atomic level, which is conducive for fast electron transfer.[35,36] Besides, abundant active edge sites with desirable electronic structures can be provided for altering the reaction mechanisms.[37,38] On further combination with the excellent stability contributed by the robust interface, significantly reinforced electrochemical performances have been achieved by EHs, outperforming their building blocks with single components.[39,40]

As an emerging but fast-rising field, numerous breakthroughs have been witnessed in recent years, while a dedicated review is still lacking. Herein, we provide a timely summary on the latest advances in the rational design of EHs for electrochemical applications (Scheme 1). The synthesis strategies of EHs are first outlined with a focus on how to rationally integrate different components. Secondly, the advantages of EHs in electrochemical applications are highlighted with the structure–property relationship elucidated. Finally, our perspectives on the challenges and future opportunities in this field are provided.

Chao Liu received his Bachelor (2012) and Ph.D. degrees (2018) from Nanjing University of Science and Technology. He worked as a postdoctoral fellow in Prof. Chengzhong Yu's group at East China Normal University (2018–2021). He is currently a professor at East China Normal University. His research focuses on the design and synthesis of novel nanostructured materials for catalysis.

2. Synthesis strategies for the formation of EHs

Inspired by the appealing features, great efforts have been devoted to the construction of EHs for electrochemical applications. The basic concept is to create high-quality interfaces between different components with low lattice mismatch. To this end, diverse synthetic methods have been developed and can be briefly divided into two categories including direct one-step and indirect two-step synthesis. The detailed processes will be discussed in the following sections.

2.1 Direct one-step synthesis

The one-step synthesis is generally performed by adding all the precursors in one pot followed by a hydro or solvothermal treatment using water or organic solvents as the reaction medium. During the reaction process, the EHs are directly formed by growth of different components sharing one interface, where the selection of appropriate conditions (*e.g.* reaction temperature, reactant concentration and ratio of different precursors) is desired. For example, using $Pt(acac)_2$ and $Ru(acac)_2$ as precursors with a mass ratio of 2.86/1, a cubic PtRu/Ru EH could be directly synthesized in oleylamine and oleic acid mixed solution by a controlled heating process.[41] When the Ru precursor was insufficient, only the PtRu alloy could be obtained. Apart from noble metals, the synthesis of transition metal based EHs was also reported by Lin and coworkers. NiSe/Ni_3S_2 heterostructures could be prepared by immersion of Ni foam as a metal source in a solution of Se, S and diethylenetriamine followed by a solvothermal reaction at 160 °C.[42] The NiSe/Ni_3S_2 ratio in the heterostructure could be facilely tuned by adjusting the Se/S feeding ratio.

Eventhough simple and easy to perform, the one-step synthesis toward EHs has been realized only in few examples. Furthermore, elaborate structure design is hardly achieved due to the difficulty in control over the growth and combination manners of different components in one complex system.

2.2 Indirect two-step synthesis

For the two-step process, one material is synthesized in the first step as a substrate followed by a second-step addition of precursors for inducing the formation of another component on the surface or in the skeleton by interfacial growth or post-conversion. Notably, the two-step process has much wider application range than the one-step process. To date, a plenty of materials including metal compounds (*e.g.* metal oxides,[40] metal hydroxides,[43] metal sulfides,[44] metal selenides,[45] and metal–organic frameworks[46]) and carbon-based materials have been employed as substrates for further growth of EHs.

2.2.1 Epitaxial growth. Epitaxial growth, as one of the most frequently used pathways toward EHs, involves the oriented

© 2023 The Author(s). Published by the Royal Society of Chemistry

Open Access Article. Published on 29 11 2022. Downloaded on 2026-06-01 2:54:26.
This article is licensed under a Creative Commons Attribution-NonCommercial 3.0 Unported Licence.

deposition of a crystalline material on the surface of another crystalline substrate with a high degree of crystallographic alignment.[47,48] To realize the epitaxial growth, a small lattice mismatch between two crystals is vital, which can minimize the interfacial energy of resultant heterostructures. For instance, using SnO_2 nanowires presynthesized on stainless steel as starting materials, FeOOH nanorods were grown on the surface by reaction with $FeCl_3$ and $NaNO_3$ through a hydrothermal treatment at 100 °C.[49] As a result, the FeOOH/SnO_2 EH with six-fold-symmetry branched architecture was formed, where the lattice mismatch between the two components was only 4.6%. Through further calcination in air, the α-Fe_2O_3/SnO_2 EH with well-preserved morphology could be further obtained. Under more mild conditions, EHs can also be fabricated. A typical example is the fabrication of a peony-like Ni/Co-LDH (LDH = layered double hydroxide) EH by first synthesis of Ni-LDH as seeds and sequential epitaxial growth of Co-LDH at room temperature using Ni^{2+} and Co^{2+} as metal precursors and 2-methylimidazole as the OH^- donor.[50]

As a recently emerging methodology, electrodeposition provides a facile and low-cost platform for constructing EHs in solution.[51] The reaction can be completed in even several minutes with the assistance of an external electric field. Taking carbon nanotube (CNT)@MnO_2/carbon fiber paper (CFP) as an example, flexible CFP as a current collector was immersed into CNT/$MnSO_4$/H_2SO_4 solution.[52] By a 5 min reaction, the MnO_2 nanosheets were epitaxially grown on the surface of carbon fiber with CNT incorporated, leading to the final products. Electrosynthesis has received more and more attention for fabrication of nanostructures or microscopical films. However, the application in creating EHs is obviously rarer compared to traditional wet-chemical routes.

2.2.2 Partial conversion. Apart from epitaxial growth, EHs can also be prepared by partial conversion of pre-synthesized seeds. Different from epitaxial growth requiring high structural robustness of substrates, the pre-formed seeds serve as sacrificial templates during post-conversion, providing metal sources for the formation of another component by a second-step reaction. In 2020, Sun *et al.* constructed a $NiSe_2$/$Ni(OH)_2$ EH by partial conversion of $NiSe_2$.[45] During the synthesis, $NiSe_2$ nano-octahedra were first prepared. Through further hydrothermal treatment in KOH solution, the hydrolysis of $NiSe_2$ led to the growth of $Ni(OH)_2$ on the external surface, forming the $NiSe_2$/$Ni(OH)_2$ EH with core–shell morphology. Moreover, the conversion degree of $NiSe_2$ as well as the content of $Ni(OH)_2$ could be simply altered by changing the reaction time. Aside from the hydrothermal reaction, high-temperature pyrolysis is also a highly useful route for constructing EHs by partial conversion. Generally, pyrolysis in different atmospheres (*e.g.* Ar, H_2, PH_3 and sublimed sulfur) can acquire heterostructures with different compositions (*e.g.* carbon-based materials, metal oxides, metal phosphides and metal sulfides). For example, a graphene@SiC EH was obtained by thermal decomposition of SiC at 1500 °C in an inert argon atmosphere.[53] When changing the atmosphere into mixed N_2/H_2, Fe–MoO_2/MoO_3 EH arrays on Ni foam (NF) was fabricated *via* pyrolyzing Fe–Mo/NF as the precursor.[54] Recently, Gong and coworkers used PH_3 decomposed by NaH_2PO_2 to react with (Co, Ni)–La hydroxide/NF composites at 400 °C, generating a $(Co, Ni)_2P$–La/NF EH *via* a phosphidation treatment.[55] Similarly, the N–$NiMoO_4$/NiS_2 nanowires/nanosheet EH was also synthesized by using a S containing atmosphere.[56] For the partial conversion strategy, carefully controlling the reaction conditions to avoid over-conversion is the key.

Collectively, two-step synthesis, even more complicated compared to the one-step strategy, is more controllable and efficient, enabling the synthesis of EHs with various architectures and compositions.

3. Applications in electrochemistry

To date, EHs have been widely applied in a variety of electrochemical applications due to the distinctive structural features from the rational combination of diverse components with elaborately designed interfaces such as accelerated electron transfer, boosted robustness, tunable electronic structures and so on. In this section, we will outline the promising applications of EHs in three important electrochemical fields including electrocatalysis, supercapacitors and batteries.

3.1 Electrocatalysis

3.1.1 HER/OER/water splitting. Hydrogen plays an important role in the future energy system owing to the zero emission and pollution-free features. The evolution of hydrogen from water by water splitting is a hot topic in the research community.[57,58] Recent advances have demonstrated the superiorities of EHs as electrocatalysts for the HER. In 2019, Sun *et al.* synthesized a core–shell MoS_2/CoS_2 EH on CFP through the epitaxial growth of MoS_2 nanosheets on CoS_2 nanorods (Fig. 1a).[59] In the heterostructure, the exposed active edge planes at the interface of MoS_2/CoS_2 could provide abundant active sites (Fig. 1b). The higher Femi level of CoS_2 than MoS_2 caused the spontaneous transport of electrons across the interface *via* an ohmic contact. This also led to a nucleophilic region around MoS_2 but an electrophilic region around CoS_2. Because of the difference in electronegativity, the negative O and positive H in the polar water molecule would be attracted by CoS_2 and MoS_2 respectively, facilitating the cleavage of O–H bonds and therefore promoting the HER process (Fig. 1c and d). As a result, the MoS_2/CoS_2 heterostructure exhibited a lower overpotential of 94 mV at 10 mA cm^{-2} and Tafel slope of 69.4 mV dec^{-1} (Fig. 1e and f) than individual MoS_2 (231 mV, 105.1 mV dec^{-1}) and CoS_2 (282 mV, 125.7 mV dec^{-1}).

The OER is a four-electron reaction that normally requires a very large overpotential, limiting its practical applications.[60–62] To overcome this bottleneck, Tang and coworkers reported the CeO_x/CoS@L-CeO_2 core–shell nanorods (NRs) with a Chinese tanghulu-like morphology as an efficient OER electrocatalyst, using L-CeO_2 as a hard template and ZIF-67 as a sacrificial substrate (Fig. 2a).[63] To demonstrate the advantages of the CeO_x/CoS@L-CeO_2 EH, CeO_x/CoS@S–CeO_2NRs without intergranular interfaces were fabricated by growth of only one single CeO_x/CoS hollow cage on shorter CeO_2NRs. The electrochemical

Open Access Article. Published on 29 11 2022. Downloaded on 2026-06-01 2:54:26.
This article is licensed under a Creative Commons Attribution-NonCommercial 3.0 Unported Licence.

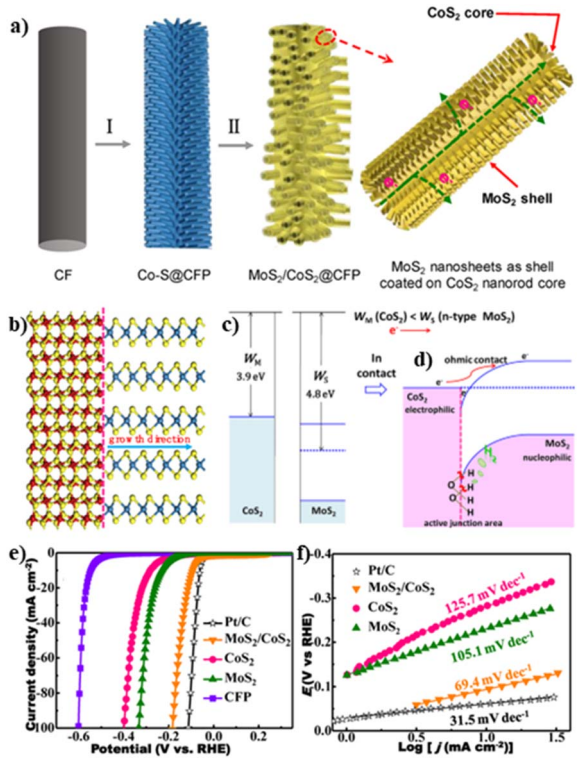

Fig. 1 (a) Illustration of the synthesis process of the MoS_2/CoS_2 heterostructure; (b) cartoon of the heteroepitaxial relationship between MoS_2 and CoS_2. The yellow, blue, and red balls represent S, Mo, and Co elements, respectively; schematic diagram for (c) the band structure of CoS_2 and n-type MoS_2 before contact and (d) the ohmic contact and the charge transfer between CoS_2 and MoS_2; (e) polarization curves and (f) Tafel plots of different samples. Reproduced with permission from ref. 59. © American Chemical Society, 2020.

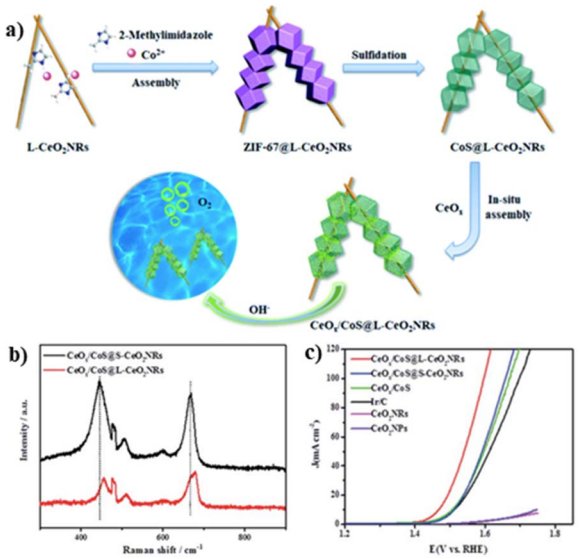

Fig. 2 (a) Scheme of the fabrication process of CeO_x/CoS@L-CeO_2-NRs; (b) Raman spectra of CeO_x/CoS@L-CeO_2NRs and CeO_x/CoS@S–CeO_2NRs; (c) LSV curves of different electrocatalysts. Reproduced with permission from ref. 63. © Royal Society of Chemistry, 2019.

results demonstrated significantly enhanced OER activity of CeO_x/CoS@L-CeO_2 with a low overpotential of 238 mV at 10 mA cm^{-2}, outperforming CeO_x/CoS@S–CeO_2NRs (269 mV at 10 mA cm^{-2}) and even commercial Ir/C (280 mV at 10 mA cm^{-2}) (Fig. 2c). The superior OER activity was attributed to the lattice strain and high-energy interfaces (Fig. 2c) by the epitaxial compression growth of CeO_x/CoS units. The lattice strain offered more disordered lattice in the CoS network with more lattice defects and vacancy sites (Fig. 2b). Together with the high-energy interface originating from the well-defined Co–S–O–Se interfaces, active sites with higher activity and exposure rate were produced for the OER process.

Furthermore, Yan and coworkers reported a $NiPS_3/Ni_2P$ heterostructure as a bifunctional electrocatalyst for both the HER and OER.[44] As presented in Fig. 3a, the lattice constant of (001) facets of $NiPS_3$ well matched with that of the rhombic unit derived from the (001) facets of hexagonal Ni_2P, enabling the epitaxial growth of Ni_2P on $NiPS_3$ along the [001] direction. The density functional theory (DFT) calculations showed that the adsorption energy of H (ΔG_{H^*}) for the NiP_3/Ni_2P heterostructure was lower than that of single $NiPS_3$ and Ni_2P, contributing to higher HER activity (Fig. 3b). Besides, the charge density difference between $NiPS_3$ and Ni_2P resulted in the formation of a built-in electric field, thus promoting the electron transfer at the interface (Fig. 3c). As a consequence, $NiPS_3/Ni_2P$ showed the lowest overpotential (20 mV at 10 mA cm^{-2} in the HER and 260 mV at 20 mA cm^{-2} in the OER) compared to $NiPS_3$ (230 mV, 370 mV) and Ni_2P (96 mV, 470 mV) in both the HER and OER (Fig. 3e and f), revealing excellent electrocatalytic properties.

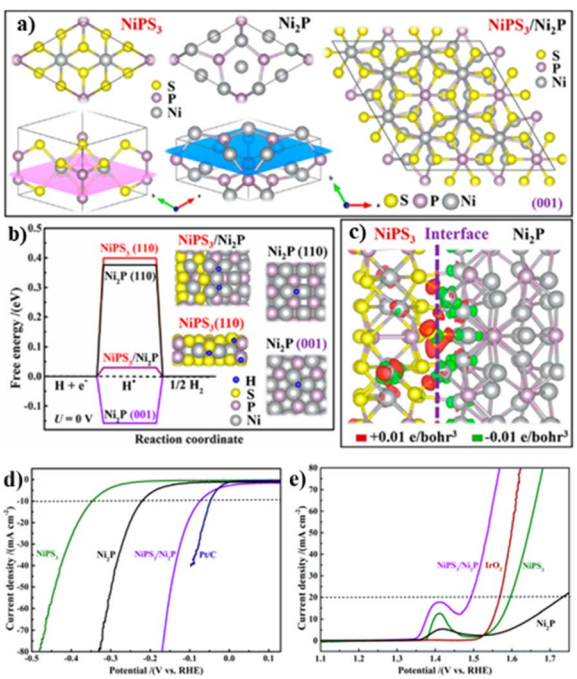

Fig. 3 (a) Graphical models to show the lattice match between $NiPS_3$ and Ni_2P; (b) ΔG_{H^*} calculation; (c) charge density distribution at the interface, The Ni, S, P, and H atoms are marked in gray, yellow, purple, and blue, respectively; LSV curves of (d) HER and (e) OER. Reproduced with permission from ref. 44. © American Chemical Society, 2019.

© 2023 The Author(s). Published by the Royal Society of Chemistry

Open Access Article. Published on 29 11 2022. Downloaded on 2026-06-01 2:54:26.
This article is licensed under a Creative Commons Attribution-NonCommercial 3.0 Unported Licence.

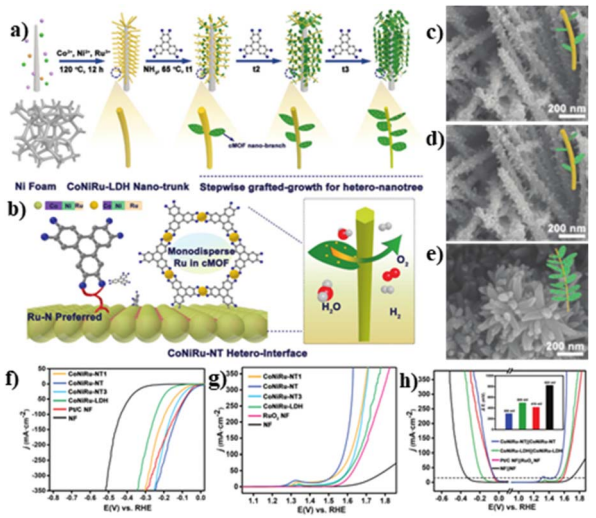

Fig. 4 (a and b) Illustration of the design of cMOF/LDH hetero-nanotree catalysts for overall water splitting; (c–e) SEM images of CoNiRu-NT 1–3; LSV curves of (f) HER, (g) OER and (h) water splitting; (h-inset) the value of ΔE of different catalysts. Reproduced with permission from ref. 64. © Wiley-VCH GmbH, 2022.

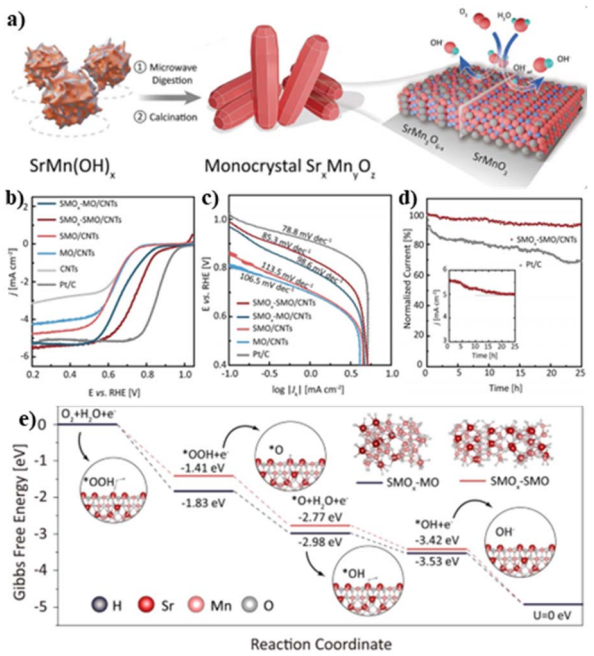

Fig. 5 (a) Scheme for the fabrication of SMO_x–SMO; (b) LSV curves; (c) Tafel slopes and (d) chronoamperometric curves for different catalysts; (e) Gibbs free energy change chart for SMO_x–SMO and SMO_x–MO. Reproduced with permission from ref. 43. © Wiley-VCH GmbH, 2021.

Beyond the half reactions of HER and OER, the investigation of EHs in the overall water splitting has also been performed. A typical example is the CoNiRu nano-tree (CoNiRu-NT) synthesized by integration of conductive MOF (cMOF) with CoNiRu-LDH supported by Ni foam (Fig. 4a).[64] By means of the multiple matches of the lattice metrics, cMOF was uniformly grafted onto the CoNiRu-LDH by heteroepitaxial growth (Fig. 4b). The EHs obtained from different reaction times were denoted as CoNiRu-NT1 (48 h), -NT (65 h), and -NT3 (85 h), with gradually increased amount of cMOF (Fig. 4c–e). The electrochemical results showed that CoNiRu-NT displayed excellent catalytic activity with low HER and OER overpotentials of 22 mV at 10 mA cm^{-2} and 255 mA at 20 mA cm^{-2}, respectively, superior to CoNiRu-NT1/3, CoNiRu-LDH and commercial RuO_2 (Fig. 4f and g). Afterwards, a two-electrode electrolytic cell was employed to investigate the practical bifunctional catalytic performance for water splitting. The ΔE value for CoNiRu-NT (Fig. 4h) was determined to be ~300 mV at 20 mA cm^{-2}, which is much lower than that of CoNiRu-LDH (500 mV), Pt/C + RuO_2 (416 mV), and NF substrates (823 mV). The performance enhancement was ascribed to the following reasons by the authors. Firstly, the introduction of cMOF provided excellent electrical conductivity and the nano-tree morphology increased the specific surface area for mass transfer. Secondly, the generated heterointerface with strong electric interconnection promoted the exposure of active sites, further accelerated the electron transfer and enhanced the structural robustness during electrocatalysis.

3.1.2 ORR. The ORR, where O_2 is reduced to H_2O/OH^-, is a key electrochemical reaction in fuel cells and metal-air batteries, while suffers from sluggish kinetics due to the multistep reaction mechanism.[65,66] EHs have recently been demonstrated as high-performance electrocatalysts with enhanced ORR activity and selectivity. In 2021, the Liu group investigated the ORR performance of the $SrMn_3O_{6-x}$@$SrMnO_3$ (SMO_x–SMO) EH synthesized by a sequential micro-wave digestion–calcination process.[43] The epitaxial growth of $SrMnO_3$ on $SrMn_3O_{6-x}$ relied on great Sr enrichment ability of lattice Sr in the inner layer SMO_x (Fig. 5a). To better understand the superiority of the EH, a control sample of $SrMn_3O_{6-x}$@Mn_3O_4 (SMO_x–MO) without an epitaxial interface was also designed. As shown in Fig. 5b, SMO_x–SMO exhibited superior ORR activity ($E_{1/2}$ = 0.74 V and j of −5.46 mA cm^{-2} at 0.2 V) to SMO_x–MO (0.67 V, −5.24 mA cm^{-2}), SMO (0.64 V, −4.76 mA cm^{-2}) and MO (0.65 V, −4.42 mA cm^{-2}). Furthermore, SMO_x–SMO had the lowest Tafel slope, indicating the fastest ORR kinetics (Fig. 5c). Compared to commercial Pt/C, SMO_x–SMO also showed better cycle stability (Fig. 5d). The possible reasons for enhanced ORR performances of SMO_x–SMO were the optimized electronic structures with weakened adsorption of intermediate *O and promoted desorption of *OH (Fig. 5e).

3.1.3 NRR. The electrochemical N_2 reduction reaction (NRR) is one of the most efficient methods for the synthesis of NH_3, where the design of high-performance electrocatalysts is the key.[67,68] In 2021, Shi and co-workers reported a $Cu_{2-x}S/MoS_2$ EH for the electrocatalytic NRR *via* epitaxial growth of a thin MoS_2 layer on $Cu_{2-x}S$ quantum dots.[69] In the EH, the Cu^{2+} $2p_{3/2}$ shifted to lower binding energy with increased electron density by the interfacial electron transfer from Mo to Cu, providing active sites with high activity and selectivity. As a result, improved NRR performances with an NH_3 yield of 22.1 μg h^{-1} mg^{-1} and a Faraday efficiency of 6.06% at −0.5 V were achieved.

© 2023 The Author(s). Published by the Royal Society of Chemistry

Open Access Article. Published on 29 11 2022. Downloaded on 2026-06-01 2:54:26.
This article is licensed under a Creative Commons Attribution-NonCommercial 3.0 Unported Licence.

3.2 Supercapacitors

Supercapacitors, also known as electrochemical capacitors, have appealing characteristics of high-power density, long cycle life and low maintenance cost. The performance of supercapacitors is predominately determined by the structures of electrode materials.[70,71] Recently, EHs have been highlighted as an attractive family of electrode materials for supercapacitors. In 2020, Ma *et al.* reported the growth of a CNT@MnO_2/CFP EH on CFP as an electrode material for supercapacitors.[52] Due to the 3D interconnected network with high conductivity and the strong interfacial interaction between the CNT and MnO_2, CNT@MnO_2/CFP with optimized CNT content possessed the longest charge–discharge time and smallest decline of specific capacitances by increasing the current density, delivering outstanding capacitance and rate capability.

In addition to the carbon/metal oxide composites, Sun and coworkers reported a $NiSe_2$/$Ni(OH)_2$ EH synthesized by a epitaxial-like strategy for supercapacitors (Fig. 6a).[45] The epitaxial-like growth of $Ni(OH)_2$ on $NiSe_2$ led to the formation of a core–shell $NiSe_2$/$Ni(OH)_2$ heterojunction with an octahedral shape (Fig. 6b). Thanks to the facilitated electron transfer around the interface, the heterostructures exhibited a long charge–discharge time with a high capacity up to 909 C g^{-1} for the optimized $NiSe_2$/$Ni(OH)_2$-2h (Fig. 6c).

Beyond above studies on binary heterostructures, construction of ternary epitaxial structures offers more opportunities to enhance the performance. One classical example is the self-supporting NiSe/Ni_3S_2/$Ni_{12}P_5$ EH on Ni foam demonstrated by Lin *et al.*[42] As shown in Fig. 6d and e, the ternary NiSe/Ni_3S_2/$Ni_{12}P_5$ exhibited remarkable supercapacitor performances with longer charge–discharge time, larger capacity (2.04 mA h cm^{-2}), and better cycle stability (after 2000 cycles, 96% of the original capacity retained) than the samples with unitary and binary components. Within the heterostructure, the electron densities were re-distributed, simultaneously enhancing the electron transfer and structural stability. Upon further combination with the higher conductivity of $Ni_{12}P_5$, improved properties were eventually achieved.

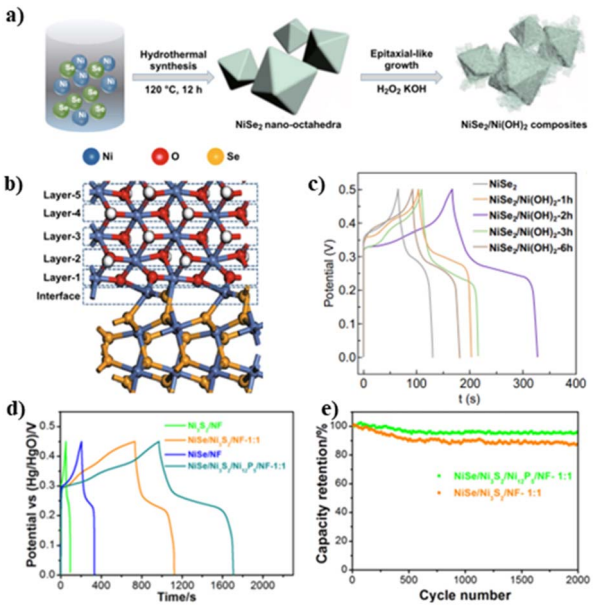

Fig. 6 (a) Synthetic process of the $NiSe_2$/$Ni(OH)_2$ heterostructure; (b) cartoon of the heterointerface; (c) GCD curves of different catalysts; reproduced with permission from ref. 45. © Springer Nature, 2020. (d) GCD curves at 10 mA cm^{-2} and (e) 2000 GCD cycles of the NiSe/Ni_3S_2/$Ni_{12}P_5$ heterostructure and control samples. Reproduced with permission from ref. 42. © Elsevier, 2018.

3.3 Batteries

Batteries including lithium-ion batteries (LIBs), sodium-ion batteries (SIBs) and potassium-ion batteries (PIBs), *etc.* have been considered as one of the most promising devices for energy storage and conversion due to their high theoretical energy density and specific capacity, long cycle life and light weight.[72,73] Nevertheless, it still remains a great challenge to design suitable electrode materials for LIBs, SIBs and PIBs toward satisfactory implementation.

3.3.1 LIBs. As the most commercialized battery technology, the investigation on electrode materials for LIBs is of great significance.[74–76] For example, Fan *et al.* reported an epitaxial α-Fe_2O_3/SnO_2 heterostructure with improved LIB performance.[49] Starting from SnO_2 rods, the Fe_2O_3/SnO_2 EH with well-matched

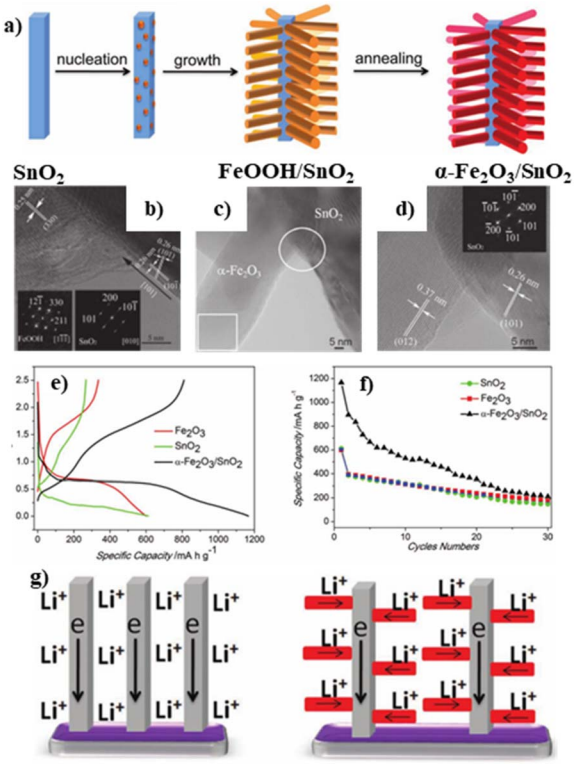

Fig. 7 (a) Scheme showing the formation process of α-Fe_2O_3/SnO_2 heterostructures; HRTEM image of (b) FeOOH/SnO_2, (c and d) α-Fe_2O_3/SnO_2; (e) first charge–discharge profiles at a current density of 1000 mA g^{-1}; (f) cycling performance of different samples; (g) schematic comparison of the unidirectional nanowires and branched nanostructures for Li and electron transfer. Reproduced with permission from ref. 49. © Wiley-VCH GmbH, 2011.

© 2023 The Author(s). Published by the Royal Society of Chemistry

Open Access Article. Published on 29 11 2022. Downloaded on 2026-06-01 2:54:26.
This article is licensed under a Creative Commons Attribution-NonCommercial 3.0 Unported Licence.

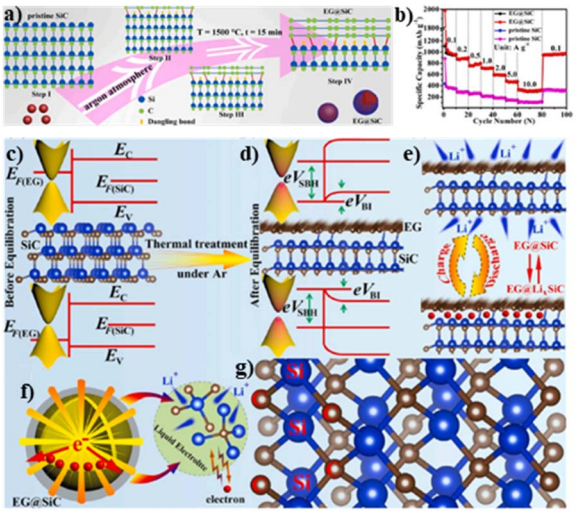

Fig. 8 (a) Schematic illustration of the synthesis of EG@SiC; (b) comparison of the specific capacities of EG@SiC and pristine SiC anodes at various rates; schemes of the band structures in EG and EG@SiC (c) before and (d) after equilibration; (e) discharge and charge processes; (f) electrochemical kinetic process and (g) the strong interaction between EG and SiC. Reproduced with permission from ref. 53. © Elsevier, 2020.

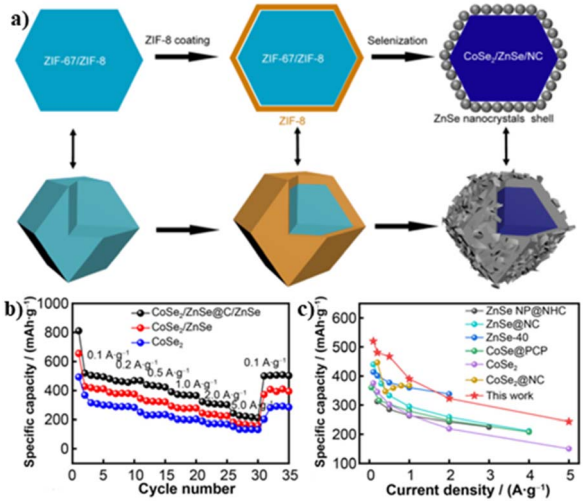

Fig. 9 (a) Synthetic process of $CoSe_2$/ZnSe/NC@ZnSe/NC; (b) rate capacity of $CoSe_2$/ZnSe/NC@ZnSe/NC, $CoSe_2$/ZnSe and $CoSe_2$; (c) comparison of rate capacity with other reported anode materials. Reproduced with permission from ref. 79. © Springer Nature, 2022.

interface was obtained by calcination of FeOOH/SnO_2 as an intermediate (Fig. 7a–d). During the Li storage process, α-Fe_2O_3/SnO_2 showed a remarkably improved initial discharge capacity of 1167 mA h g^{-1}, almost twofold of SnO_2 (612 mA h g^{-1}) and α-Fe_2O_3/SnO_2 (598 mA h g^{-1}, Fig. 7e). Apart from that, α-Fe_2O_3/SnO_2 also exhibited better cycling performance with high electrochemical stability (Fig. 7f). This enhancement was caused by the robust interface between α-Fe_2O_3 and SnO_2, and highly utilized active sites by the branched structure (Fig. 7g).

More recently in 2020, Zhang and coworkers reported a graphene@SiC EH as a high-performance anode for LIBs (Fig. 8a).[53] The heterostructure gave rise to a built-in electric field for the charge transportation by forming a Schottky junction with surface energy band bending (Fig. 8c and d). The highly exposed interface provided fast pathways for the intercalation/deintercalation of Li ions (Fig. 8e). In addition, the thermal decomposition process resulted in the tight contact between SiC and graphene, allowing for rapid charge collection and transportation (Fig. 8f). The strong interfaces with high surface electron densities could efficiently reduce the Li^+ diffusion energy barrier during the lithiation/delithiation processes (Fig. 8g). Based on these advantages, the heterostructure could retain an excellent reversible capacity of 332.1 mA h g^{-1} at a high current density of 10 A g^{-1}, superior to the pristine SiC (Fig. 8b).

3.3.2 SIBs/PIBs. Compared to LIBs, SIBs and PIBs exhibit merits of high system safety, abundant resources and low cost.[77,78] Considering the similar working principles of SIBs/PIBs to LIBs, improved performances are also expected to be achieved by using EHs as SIB/PIB electrode materials. For example, a core–shell $CoSe_2$/ZnSe/NC@ZnSe/NC (NC=N-doped carbon) EH was synthesized by Lu and coworkers (Fig. 9a) using ZIF-67@ZIF-8 hybrid MOFs as precursors.[79] The small degree of lattice mismatch between $CoSe_2$ and ZnSe was conducive for creating the epitaxial interface. Benefiting from the heterogeneous structure with enhanced conductivity and reduced capacity decline, $CoSe_2$/ZnSe/NC@ZnSe/NC showed higher specific capacity at each current density. A specific capacity of 509.3 mA h g^{-1} could be achieved when the current density returned back to 0.1 A g^{-1} (Fig. 9b), exceeding other anode materials (Fig. 9c). Using a similar synthetic method, the same group also synthesized CoS_2/Sb_2S_3@NC/CNT heterostructures as electrode materials for PIBs.[80] The resultant composites showed excellent cycling stability with a reversible specific capacity of 453.5 mA h g^{-1} at a current density of 0.2 A g^{-1} after 50 cycles, which may have resulted from the synergistic effects between CoS_2 and Sb_2S_3.

4. Conclusions and outlook

In summary, this Minireview provides an overview of the recent advances in EHs with a focus on the synthetic strategies and electrochemical applications. Although significant advances have been achieved, the development of EH-based electrode materials is perhaps still in its infancy and there are still several challenges in this field for further investigation, especially regarding the structure design, synthesis methodology and applications.

(1) The controlled synthesis of EHs with desirable structures and compositions is in demand, which is crucial for tuning properties. Currently reported EHs mainly exhibit simple solid structures with limitations in diffusion related processes for example electrochemical applications. The rapid development of nanoscience has produced various innovative structures for reinforcing diffusion such as hollow,[81,82] yolk–shell[83,84] and open-frame like structures,[85,86] which however have rarely been

Open Access Article. Published on 29 11 2022. Downloaded on 2026-06-01 2:54:26.
This article is licensed under a Creative Commons Attribution-NonCommercial 3.0 Unported Licence.

achieved in EHs. Apart from that, precise organization of the spatial distribution of different components in EHs toward for example complex janus architectures remains largely unexplored. Beyond the nanoscale level, more efforts are suggested to be devoted to the growth of EHs on flexible substrates. Apart from architecture, the composition of EHs is predominately limited in binary systems. Merging more types of components into one EH will enrich the interface diversities for various applications.

(2) To address these issues, a major challenge is to develop new synthetic methodologies that can elaborately regulate the growth and combination manners of different crystal units. Developing advanced manufacture strategies such as site-selective etching, conversion and growth by utilizing the facet-dependent features of crystal substrate is worthy of investigation. On this basis, EHs of complex nanostructures are expected to be created. To construct flexible EHs, substrates such as polymer and carbon-based fibers or membranes are recommended. In this regard, combination of the electrospinning technique with EH growth is a useful route. MOFs as a novel kind of crystalline porous material can facilely incorporate various metal elements with high dispersion in one framework. Thus, using MOFs as precursors, polynary EHs may be facilely obtained by post thermal and/or chemical treatment.

(3) From the application point of view, in-depth understanding on the underlying structure–performance relationship of EHs in electrochemical applications is highly desired. *In situ* characterization techniques such as Raman spectroscopy,[87] infrared spectroscopy,[88] X-ray photoelectron spectroscopy,[89] X-ray diffraction[90] and TEM[91] are powerful tools for monitoring the composition and structure evolution during electrochemical processes. Besides, the applications of EHs in recently emerging fields such as CO_2 reduction, H_2O_2 production, *etc.* are of great significance.

Collectively, EHs play an important role in modulating the composition, structure and thus properties of various materials. With continued efforts of the research community and development of the EH field, more rational and general approaches have to be developed to manipulate the controlled synthesis of EHs, and thus to serve for applications with enhanced performances. It is believed that many exciting results related to EHs will be achieved in the near future.

Conflicts of interest

There are no conflicts to declare.

Acknowledgements

The authors acknowledge support from the National Natural Science Foundation of China (NSFC 51908218 and 21905092), Scientific Research Foundation of Shanghai Institute of Technology (10120K226156-A06-YJ2022-62), and the Key Laboratory of Jiangsu Province for Chemical Pollution Control and Resources Reuse (Nanjing University of Science and Technology).

References

1 W. Li, J. Liu and D. Zhao, *Nat. Rev. Mater.*, 2016, **1**, 16023.
2 Y. Liu, F. Liu, N. Ding, X. Hu, C. Shen, F. Li, M. Huang, Z. Wang, W. Sand and C.-C. Wang, *Chin. Chem. Lett.*, 2020, **31**, 2539–2548.
3 H. Zhang, W. Zhou, T. Chen, B. Y. Guan, Z. Li and X. W. Lou, *Energy Environ. Sci.*, 2018, **11**, 1980–1984.
4 X.-P. Li, L.-R. Zheng, S.-J. Liu, T. Ouyang, S. Ye and Z.-Q. Liu, *Chin. Chem. Lett.*, 2022, **33**, 4761–4765.
5 W. Sheng, Z. Zhuang, M. Gao, J. Zheng, J. G. Chen and Y. Yan, *Nat. Commun.*, 2015, **6**, 5848.
6 X. Tian, P. Zhao and W. Sheng, *Adv. Mater.*, 2019, **31**, 1808066.
7 B. Zhu, R. Zou and Q. Xu, *Adv. Energy Mater.*, 2018, **8**, 1801193.
8 Z. P. Ifkovits, J. M. Evans, M. C. Meier, K. M. Papadantonakis and N. S. Lewis, *Energy Environ. Sci.*, 2021, **14**, 4740–4759.
9 H. Sun, Z. Yan, F. Liu, W. Xu, F. Cheng and J. Chen, *Adv. Mater.*, 2020, **32**, e1806326.
10 H. Wang, S. Zhu, J. Deng, W. Zhang, Y. Feng and J. Ma, *Chin. Chem. Lett.*, 2021, **32**, 291–298.
11 B. Zhang, Y. Zheng, T. Ma, C. Yang, Y. Peng, Z. Zhou, M. Zhou, S. Li, Y. Wang and C. Cheng, *Adv. Mater.*, 2021, **33**, e2006042.
12 Y. Shao, M. F. El-Kady, L. J. Wang, Q. Zhang, Y. Li, H. Wang, M. F. Mousavi and R. B. Kaner, *Chem. Soc. Rev.*, 2015, **44**, 3639–3665.
13 G. Wang, L. Zhang and J. Zhang, *Chem. Soc. Rev.*, 2012, **41**, 797–828.
14 X. Zhao, L. Mao, Q. Cheng, J. Li, F. Liao, G. Yang, L. Xie, C. Zhao and L. Chen, *Chem. Eng. J.*, 2020, **387**, 124081.
15 W. Lee, J. Kim, S. Yun, W. Choi, H. Kim and W.-S. Yoon, *Energy Environ. Sci.*, 2020, **13**, 4406–4449.
16 F. Ming, H. Liang, G. Huang, Z. Bayhan and H. N. Alshareef, *Adv. Mater.*, 2021, **33**, e2004039.
17 G. D. Park, J. S. Park, J. K. Kim and Y. C. Kang, *Adv. Energy Mater.*, 2021, **11**, 2003058.
18 M. Wang, D. Yin, Y. Cao, X. Dong, G. Gao, X. Hu, C. Jin, L. Fan, J. Yu and H. Liu, *Chin. Chem. Lett.*, 2022, **33**, 4350–4356.
19 H. Sun, J. Zhu, D. Baumann, L. Peng, Y. Xu, I. Shakir, Y. Huang and X. Duan, *Nat. Rev. Mater.*, 2018, **4**, 45–60.
20 Y. Tang, Y. Zhang, W. Li, B. Ma and X. Chen, *Chem. Soc. Rev.*, 2015, **44**, 5926–5940.
21 X. Yin, S. Sarkar, S. Shi, Q. A. Huang, H. Zhao, L. Yan, Y. Zhao and J. Zhang, *Adv. Funct. Mater.*, 2020, **30**, 1908445.
22 Y. Xu, Z. Lin, X. Zhong, B. Papandrea, Y. Huang and X. Duan, *Angew. Chem., Int. Ed.*, 2015, **54**, 5345–5350.
23 A. Yu, G. Ma, L. Zhu, Y. Hu, R. Zhang, H.-Y. Hsu, P. Peng and F.-F. Li, *Nanoscale*, 2021, **13**, 15973–15980.
24 L. Wang, H. Liu, J. Zhao, X. Zhang, C. Zhang, G. Zhang, Q. Liu and H. Duan, *Chem. Eng. J.*, 2020, **382**, 122979.
25 X. Hu, Z. Sun, G. Mei, X. Zhao, B. Y. Xia and B. You, *Adv. Energy Mater.*, 2022, **12**, 2201466.

© 2023 The Author(s). Published by the Royal Society of Chemistry

Open Access Article. Published on 29 11 2022. Downloaded on 2026-06-01 2:54:26.
This article is licensed under a Creative Commons Attribution-NonCommercial 3.0 Unported Licence.

26 Y. Cao, S. Guo, C. Yu, J. Zhang, X. Pan and G. Li, *J. Mater. Chem. A*, 2020, **8**, 15767–15773.
27 X. Y. Yu and X. W. David Lou, *Adv. Energy Mater.*, 2018, **8**, 1701592.
28 Y. Li, Z. Dong and L. Jiao, *Adv. Energy Mater.*, 2019, **10**, 1902104.
29 X. Xia, L. Wang, N. Sui, V. L. Colvin and W. W. Yu, *Nanoscale*, 2020, **12**, 12249–12262.
30 J. Chen, Q. Ma, X. J. Wu, L. Li, J. Liu and H. Zhang, *Nano-Micro Lett.*, 2019, **11**, 86.
31 Z. Fan and H. Zhang, *Acc. Chem. Res.*, 2016, **49**, 2841–2850.
32 J. Qiao, X. Zhang, C. Liu, L. Lyu, Y. Yang, Z. Wang, L. Wu, W. Liu, F. Wang and J. Liu, *Nano-Micro Lett.*, 2021, **13**, 75.
33 C. Tan, J. Chen, X.-J. Wu and H. Zhang, *Nat. Rev. Mater.*, 2018, **3**, 17089.
34 D. Xu, Y. Yang, K. Le, G. Wang, A. Ouyang, B. Li, W. Liu, L. Wu, Z. Wang, J. Liu and F. Wang, *Chem. Eng. J.*, 2021, **417**, 129350.
35 Y. Zhao, Y. Zhang, H. Zhao, X. Li, Y. Li, L. Wen, Z. Yan and Z. Huo, *Nano Res.*, 2015, **8**, 2763–2776.
36 C. Zhu, A. L. Wang, W. Xiao, D. Chao, X. Zhang, N. H. Tiep, S. Chen, J. Kang, X. Wang, J. Ding, J. Wang, H. Zhang and H. J. Fan, *Adv. Mater.*, 2018, **30**, e1705516.
37 A. Singh, J. Rohilla, M. S. Hassan, T. Devaiah C, P. P. Ingole, P. K. Santra, D. Ghosh and S. Sapra, *ACS Appl. Nano Mater.*, 2022, **5**, 4293–4304.
38 L. Yang, H. Liu, Z. Zhou, Y. Chen, G. Xiong, L. Zeng, Y. Deng, X. Zhang, H. Liu and W. Zhou, *ACS Appl. Mater. Interfaces*, 2020, **12**, 33785–33794.
39 C. W. Lee, S.-D. Seo, D. W. Kim, S. Park, K. Jin, D.-W. Kim and K. S. Hong, *Nano Res.*, 2013, **6**, 348–355.
40 J. Yan, P. Xu, S. Chen, G. Wang, F. Zhang, W. Zhao, Z. Zhang, Z. Deng, M. Xu, J. Yun and Y. Zhang, *Electrochim. Acta*, 2020, **330**, 135312.
41 L. Bai, *Appl. Surf. Sci.*, 2018, **433**, 279–284.
42 K. Tao, Y. Gong and J. Lin, *Nano Energy*, 2019, **55**, 65–81.
43 C. Chen, X. T. Wang, J. H. Zhong, J. Liu, G. I. N. Waterhouse and Z. Q. Liu, *Angew. Chem., Int. Ed.*, 2021, **60**, 22043–22050.
44 Q. Liang, L. Zhong, C. Du, Y. Luo, J. Zhao, Y. Zheng, J. Xu, J. Ma, C. Liu, S. Li and Q. Yan, *ACS Nano*, 2019, **13**, 7975–7984.
45 H. Mei, Z. Huang, B. Xu, Z. Xiao, Y. Mei, H. Zhang, S. Zhang, D. Li, W. Kang and D. F. Sun, *Nano-Micro Lett.*, 2020, **12**, 61.
46 L. Gan, J. Lai, Z. Liu, J. Luo, S. Zhang and Q. Zhang, *J. Alloys Compd.*, 2022, **905**, 164200.
47 J. L. Zhang, C. Han, Z. Hu, L. Wang, L. Liu, A. T. S. Wee and W. Chen, *Adv. Mater.*, 2018, **30**, e1802207.
48 D. Zhou, H. Li, N. Si, H. Li, H. Fuchs and T. Niu, *Adv. Funct. Mater.*, 2020, **31**, 2006997.
49 W. Zhou, C. Cheng, J. Liu, Y. Y. Tay, J. Jiang, X. Jia, J. Zhang, H. Gong, H. H. Hng, T. Yu and H. J. Fan, *Adv. Funct. Mater.*, 2011, **21**, 2439–2445.
50 T. Huang, S. K. Moon and J.-M. Lee, *Electrochim. Acta*, 2019, **296**, 590–597.
51 S. Shit, S. Bolar, N. C. Murmu and T. Kuila, *Chem. Eng. J.*, 2021, **417**, 129333.
52 K. Wu, Z. Ye, Y. Ding, Z. Zhu, X. Peng, D. Li and G. Ma, *J. Power Sources*, 2020, **477**, 229031.
53 C. Sun, Y.-J. Wang, H. Gu, H. Fan, G. Yang, A. Ignaszak, X. Tang, D. Liu and J. Zhang, *Nano Energy*, 2020, **77**, 105092.
54 J. Chen, Q. Zeng, X. Qi, B. Peng, L. Xu, C. Liu and T. Liang, *Int. J. Hydrogen Energy*, 2020, **45**, 24828–24839.
55 K. Tao, H. Dan, Y. Hai, L. Liu and Y. Gong, *Inorg. Chem.*, 2020, **59**, 7000–7011.
56 L. An, J. Feng, Y. Zhang, R. Wang, H. Liu, G.-C. Wang, F. Cheng and P. Xi, *Adv. Funct. Mater.*, 2019, **29**, 1805298.
57 F. Liu, C. Shi, X. Guo, Z. He, L. Pan, Z. F. Huang, X. Zhang and J. J. Zou, *Adv. Sci.*, 2022, **9**, e2200307.
58 Z. Y. Yu, Y. Duan, X. Y. Feng, X. Yu, M. R. Gao and S. H. Yu, *Adv. Mater.*, 2021, **33**, e2007100.
59 N. Huang, Y. Ding, S. Yan, L. Yang, P. Sun, C. Huang and X. Sun, *ACS Appl. Energy Mater.*, 2019, **2**, 6751–6760.
60 Z. P. Wu, X. F. Lu, S. Q. Zang and X. W. Lou, *Adv. Funct. Mater.*, 2020, **30**, 1910274.
61 H. Yang, Y. Liu, X. Liu, X. Wang, H. Tian, G. I. N. Waterhouse, P. E. Kruger, S. G. Telfer and S. Ma, *eScience*, 2022, **2**, 227–234.
62 L. Zhang, H. Jang, H. Liu, M. G. Kim, D. Yang, S. Liu, X. Liu and J. Cho, *Angew. Chem., Int. Ed.*, 2021, **60**, 18821–18829.
63 H. Xu, Y. Yang, X. Yang, J. Cao, W. Liu and Y. Tang, *J. Mater. Chem. A*, 2019, **7**, 8284–8291.
64 Y. Wang, S. Wang, Z. L. Ma, L. T. Yan, X. B. Zhao, Y. Y. Xue, J. M. Huo, X. Yuan, S. N. Li and Q. G. Zhai, *Adv. Mater.*, 2022, **34**, e2107488.
65 C. Hu and L. Dai, *Angew. Chem., Int. Ed.*, 2016, **55**, 11736–11758.
66 W. J. Niu, J. Z. He, B. N. Gu, M. C. Liu and Y. L. Chueh, *Adv. Funct. Mater.*, 2021, **31**, 2103558.
67 J. Sun, W. Kong, Z. Jin, Y. Han, L. Ma, X. Ding, Y. Niu and Y. Xu, *Chin. Chem. Lett.*, 2020, **31**, 953–960.
68 C. Xue, X. Zhou, X. Li, N. Yang, X. Xin, Y. Wang, W. Zhang, J. Wu, W. Liu and F. Huo, *Adv. Sci.*, 2021, **9**, 2104183.
69 T. Jiang, L. Li, L. Li, Y. Liu, D. Zhang, D. Zhang, H. Li, B. Mao and W. Shi, *Chem. Eng. J.*, 2021, **426**, 130650.
70 M. Dai, D. Zhao and X. Wu, *Chin. Chem. Lett.*, 2020, **31**, 2177–2188.
71 S. Kumar, G. Saeed, L. Zhu, K. N. Hui, N. H. Kim and J. H. Lee, *Chem. Eng. J.*, 2021, **403**, 126352.
72 H. Kong, W. Cui, C. Yan, Y. Kong, C. Lv and G. Chen, *Chem. Eng. J.*, 2021, **419**, 129490.
73 X. Xu, F. Li, D. Zhang, Z. Liu, S. Zuo, Z. Zeng and J. Liu, *Adv. Sci.*, 2022, **9**, e2200247.
74 A. Huang, Y. Ma, J. Peng, L. Li, S.-l. Chou, S. Ramakrishna and S. Peng, *eScience*, 2021, **1**, 141–162.
75 B. Liu, K. Jiang, K. Zhu, X. Liu, K. Ye, J. Yan, G. Wang and D. Cao, *Chem. Eng. J.*, 2022, **446**, 137208.
76 R. Xia, K. Zhao, L. Y. Kuo, L. Zhang, D. M. Cunha, Y. Wang, S. Huang, J. Zheng, B. Boukamp, P. Kaghazchi, C. Sun, J. E. ten Elshof and M. Huijben, *Adv. Energy Mater.*, 2021, **12**, 2102972.
77 S. Liu, L. Kang, J. Henzie, J. Zhang, J. Ha, M. A. Amin, M. S. A. Hossain, S. C. Jun and Y. Yamauchi, *ACS Nano*, 2021, **15**, 18931–18973.

© 2023 The Author(s). Published by the Royal Society of Chemistry

Open Access Article. Published on 29 11 2022. Downloaded on 2026-06-01 2:54:26.
This article is licensed under a Creative Commons Attribution-NonCommercial 3.0 Unported Licence.

78 J. Peng, W. Zhang, Q. Liu, J. Wang, S. Chou, H. Liu and S. Dou, *Adv. Mater.*, 2022, **34**, e2108384.
79 H.-J. Liang, X.-T. Li, W.-Z. Zheng, Z.-T. Liu, W. Yang, Z.-L. Liu, Y.-F. Zhang, H.-S. Fan and S.-J. Lu, *Rare Met.*, 2022, **41**, 3381–3390.
80 X. Li, H. Liang, X. Liu, R. Sun, Z. Qin, H. Fan and Y. Zhang, *Chem. Eng. J.*, 2021, **425**, 130657.
81 Y. Fang, D. Luan, S. Gao and X. W. D. Lou, *Angew. Chem., Int. Ed.*, 2021, **60**, 20102–20118.
82 M. Yang, C. H. Zhang, N. W. Li, D. Luan, L. Yu and X. W. D. Lou, *Adv. Sci.*, 2022, **9**, e2105135.
83 R. Purbia and S. Paria, *Nanoscale*, 2015, **7**, 19789–19873.
84 Z. Zhang, Y. Du, Q. C. Wang, J. Xu, Y. N. Zhou, J. Bao, J. Shen and X. Zhou, *Angew. Chem., Int. Ed.*, 2020, **59**, 17504–17510.
85 J. Nai, Y. Lu, L. Yu, X. Wang and X. W. D. Lou, *Adv. Mater.*, 2017, **29**, 1703870.
86 X. Y. Yu, L. Yu, H. B. Wu and X. W. Lou, *Angew. Chem., Int. Ed.*, 2015, **127**, 5421–5425.
87 H. Q. Chen, H. Ze, M. F. Yue, D. Y. Wei, Y. A, Y. F. Wu, J. C. Dong, Y. J. Zhang, H. Zhang, Z. Q. Tian and J. F. Li, *Angew. Chem., Int. Ed.*, 2022, **61**, e202117834.
88 Y.-Y. Lou, S.-H. Yin, J. Yang, L.-F. Ji, J.-Y. Fang, S.-Q. Zhang, M.-B. Feng, X. Yu, Y.-X. Jiang and S.-G. Sun, *Chem. Eng. J.*, 2022, **446**, 137060.
89 P. Ling, J. Zhu, Z. Wang, J. Hu, J. Zhu, W. Yan, Y. Sun and Y. Xie, *Nanoscale*, 2022, **14**, 14023–14028.
90 S. Medina-Carrasco and J. M. Valverde, *Chem. Eng. J.*, 2022, **429**, 132244.
91 M. Yousaf, U. Naseer, Y. Li, Z. Ali, N. Mahmood, L. Wang, P. Gao and S. Guo, *Energy Environ. Sci.*, 2021, **14**, 2670–2707.

© 2023 The Author(s). Published by the Royal Society of Chemistry